

## Effect of Short Heat Treatment Routes on the Tribological Properties of Ti-6Al-4V Alloy

N. Nikoogoftar<sup>1</sup>, S. H. Razavi<sup>2\*</sup> and M. Ghanbari<sup>1</sup>

\* hrazavi@just.ac.ir

Received: March 2017

Accepted: August 2017

<sup>1</sup> Materials Engineering Department, Karaj Branch, Islamic Azad University, Karaj, Iran.

<sup>2</sup> School of Metallurgy and Materials Engineering, Iran University of Science and Technology, Tehran, Iran.

DOI: 10.22068/ijmse.14.3.21

**Abstract:** In this research, the effect of annealing and aging temperature as well as the effect of quenching media on the microstructure, hardness and dry sliding wear behavior of Ti-6Al-4V alloy has been studied. Cylindrical samples with the diameter of 10 mm and the height of 20mm were solutionized at 930°C and 1060°C for 600 seconds and then were quenched in the cold water and in the air. The samples were aged at different temperature of 480°C, 550°C and 610°C for 360 s to increase the hardness. Heat treated samples were tested using standard pin-on-disc test machine at the applied loads of 100, 150 and 200 N. Microstructural investigations using scanning electron microscope revealed that for the samples solutionized at 930°C and quenched in the water, the microstructure is composed of primary  $\alpha$  and high volume fraction of martensitic  $\alpha'$  phase with fine precipitated of  $\beta$  between martensitic lathes. In the case of air cooled samples, transformed  $\beta$  has also been appeared in the vicinity of primary  $\alpha$ . For the samples solutionized at 1060°C and quenched in the water, fully martensitic microstructure with fine  $\beta$  precipitates was observed. For the sample solutionized at 1060°C and air quenched, plate like  $\alpha$  and lamellar grain boundary  $\beta$  were detected. The maximum hardness value relates to the sample solutionized at 1060°C and quenched in water which is equal to 433 HV. Different wear mechanisms, including oxidative wear, scratch, and delamination occurred at the worn surfaces at different applied loads. For the samples quenched in the water, the oxidative wear mechanism governing at low applied load and oxide debris was observed as separate or compacted particles which formed in the contact between pin and steel counter face detached from the sample. At higher applied loads, delamination and scratch mechanism was also observed and metallic plate like debris was detached from the sample. Mechanically mixed layer (MML) was formed on the surface of the pin at high applied loads and for the samples with low hardness value adhesion marks were also revealed on the steel disc. The minimum weight loss in the wear test is related to the sample quenched from the 1060°C in the cold water and aged at 550 °C .

**Keywords:** Ti-6Al-4V alloy, Tribology, Heat treatment, Microstructure, Hardness.

### 1. INTRODUCTION

Titanium alloys are known as important engineering alloys which have extensive applications due to their excellent combination of high strength, low density and corrosion resistance. This alloy finds wide applications in aerospace, automotive, nuclear, chemical, marine and biomedical industries. Ti-6Al-4V alloy is a widely applied  $\alpha+\beta$  titanium alloy that only covers almost half of the entire world production of titanium alloys [1, 2]. However, Ti-6Al-4V alloy has poor wear resistance that restricts its applications, particularly in areas involving wear and friction [2, 3].

The scope of the applications for titanium alloys has been somewhat impeded owing to poor

wear resistance under abrasion and erosion conditions [2, 5–7]. For example, during the sheet forming of Ti-6Al-4V alloy using spin forming process, a steel tool is in contact with the spinning metal sheet and therefore, the surface of the material will be failed due to the wear failure. Likewise, there are many reports of the occurrence of fretting wear failure in dental implants which is a result of wear between abutment and ceramic crown in dental implant. In this case, metal debris detached from the material and will cause allergic reactions. So, the material used here should have good wear resistance against the counter face. [8]

Molinari et al. [9] studied the dry sliding wear behavior of Ti-6Al-4V alloy sliding against itself at different sliding velocities and applied loads to

confirm the low wear resistance of the alloy to plastic deformation at low loads and poor protection exerted by the surface oxide. The dominant reason for the poor wear resistance of Ti-6Al-4V alloy is due to low protection exerted by the tribo oxides. The tribo-layer of Ti-6Al-4V alloy is brittle, tended to be continuously fragmented and did not adhere to the substrate, thus presenting no protective role [10]. Alam and Haseeb [11] investigated the tribological properties of Ti-6Al-4V and Ti-24Al-11Nb alloys subjected to dry sliding wear against hardened-steel and found that the lower wear rate of Ti-6Al-4V alloy was linked to severe delamination wear. An unexpectedly high wear rate for alumina sliding against Ti-6Al-4V (pin on-disk tests) was reported by Dong and Bell [12]. Qiu et al. [13] investigated tribological characteristics of Ti-6Al-4V alloy against GCr15 under high speed and dry sliding and concluded that the low wear resistance of Ti-6Al-4V alloy was attributed to the formation of a loosened oxide layer. Magaziner et al. [12] studied wear behavior of Ti-6Al-4V under reciprocation sliding conditions and observed that the wear loss was due to the adhesion and abrasion mechanism without citing the effect of tribo-oxides.

Ti-6Al-4V alloy has a broad range of mechanical properties due to the presence of various phases in the microstructures formed via different heat treatment cycles. Common heat treatment cycles are composed of holding the sample at various solutionizing temperature ranging from 780-1060°C, quenching in a proper media such as water or air and consequently, aging in a proper temperature ranging from 480-650°C [13-18]. There is an affinity of oxygen diffusion into the surface of the alloy which causes a hard and brittle case called  $\alpha$ -case. The formation of  $\alpha$ -case reduces the machinability of the alloy and so, reducing the heat treatment time

causes better mechanical properties. [19-22] Pinke [16] reported shorter time cycles for the annealing and tempering of the alloy which reduces the formation of  $\alpha$ -case. There are few reports on the tribological properties of Ti-6Al-4V alloy and the effect of shorter heating time in the annealing and tempering process. [23-24]

While there are some reports of the application of surface mechanical treatments on the wear resistance of Ti-6Al-4V alloy [25], there are few reports on the effect of heat treatment on the wear properties of this alloy against steel counter face. In this research, wear properties of Ti-6Al-4V exposed to different heat treatment cycles was systematically studied to understand the mechanisms governing the wear failure of this alloy. The objective of this study is to determine the best heat treating cycle to reduce the wear failure of Ti-6Al-4V alloy.

## 2. EXPERIMENTAL PROCEDURE

As-received material used in this research was round bar of medical grade Ti-6Al-4V alloy. The chemical composition of the initial material was examined using optical emission spectroscopy (OES) to ensure that the standard composition is met. The chemical composition of the alloy is shown in the table 1 which met the required composition of medical grade Ti-6Al-4V titanium alloy (grade 5) according to ASTM F136 [22].

Samples with the diameter of 10 mm and the height of 20 mm were cut from the rod using wire cut technique. Heat treatment cycles were applied to the samples according to the table 2 to produce different microstructure in the alloy. Solution annealing was carried out at two different temperatures of 930°C and 1060°C in an atmospheric resistance furnace. At 930°C, the alloy is in the  $\alpha$ - $\beta$  stability region and in the case

**Table 1.** The chemical composition of the as-received material.

Element	Al	V	C	N	O	Fe	H	Ti
Wt. %	6.000	4.200	0.030	0.010	0.150	0.100	0.003	Rem.

**Table 2.** Heat treatment cycles applied to the samples in this research.

Aging Time (s)	Aging Temp. (°C)	Quenching media	Solutionizing Time (s)	Solutionizing Temp. (°C)	Sample Designation
360	480	WQ	600	930	930W480
360	550	WQ	600	930	930W550
360	610	WQ	600	930	930W610
360	480	AC	600	930	930A480
360	550	AC	600	930	930A550
360	610	AC	600	930	930A610
360	480	WQ	600	1060	1060W480
360	550	WQ	600	1060	1060W550
360	610	WQ	600	1060	1060W610
360	480	AC	600	1060	1060A480
360	550	AC	600	1060	1060A550
360	610	AC	600	1060	1060A610

of 1060 °C, the sample is completely in  $\beta$  phase region. To prevent the oxidation of the alloy and minimizing the formation of  $\alpha$ -case which formed as a result of oxygen atoms diffusion in the surface of the alloy, the holding time at solutionizing temperature was minimized to 600 s. To assess the result of quenching media on the microstructural changes in the alloy, the samples were quenched in water at room temperature and also in the air. After the quenching process, the samples were aged at 480, 550 and 610 °C for 360 s.

The microstructure of the samples was studied using scanning electron microscope (SEM-AIS2300C, Seron Tech.) equipped with EDS microanalysis. The surface of the samples was grounded using SiC abrasive paper and then polished using 0.5 micron alumina suspension. To reveal the phases formed in the microstructure, the samples were chemically etched using Kroll's reagent (92 ml distilled water, 6 ml nitric acid, 2 ml hydrofluoric acid). The Vickers hardness test was used to evaluate the hardness of the materials using Kupa hardness test machine in the applied load of 10 kg for 45 s. Pin-on-disc wear test method was used to evaluate the tribological properties of the samples. Cylindrical Ti-6Al-4V samples with the diameter of 10 mm and the height of 20 mm were used as pin and the hardened 100Cr6 steel with

the hardness of 60 RC was used as counter face. Wear test was carried out under the normal applied loads of 100, 150 and 200 N which are corresponding to 1.3, 1.9 and 2.6 MPa, respectively. The revolving disc produces the linear sliding speed of 0.3 m/s. Before the wear test, the samples and the surface of the steel disc cleaned using pure acetone. The worn surface of the samples and the debris were studied using SEM to determine the wear micro mechanisms. Friction coefficient between the sample and steel disc was measured during the wear test. The weight loss of the samples was found according to the initial and the final weight of the samples.

### 3. RESULTS AND DISCUSSION

#### 3. 1. Hardness and Microstructure

The value of Vickers hardness of the heat treated sample at different conditions is shown in the table 3. The hardness value of the as-received sample was 218 HV.

As shown in table 3, the maximum hardness value is related to the sample quenched from 1060°C in the water. For this sample fully  $\beta$  phase is achieved during the solutionizing process which was completely transformed to  $\alpha'$  martensitic phase after water quenching. So, the maximum hardness is achievable after this phase

**Table 3.** The hardness value for the sample after heat treatment.

Hardness value after aging	Hardness value after solutionizing	Sample Designation
304	289	930A480
318	289	930A550
311	289	930A610
385	374	930W480
402	374	930W550
394	374	930W610
327	299	1060A480
345	299	1060A550
335	299	1060A610
411	386	1060W480
433	386	1060W550
421	386	1060W610

transformation. On the other hand, in all cases, the maximum effect of the aging process on the hardness is occurring for the samples aged at 550°C. During the aging process, some supersaturated  $\alpha'$  phase transformed to  $\alpha$  and fine  $\beta$  precipitates which distributed uniformly in the matrix and increase the hardness of the sample. In fact, based on the Ti-6Al-4V equilibrium phase diagram, for the samples solutionized over the  $\beta$  stability temperature (i.e. 1060°C), the entire matrix converted to  $\beta$  phase. During the cooling process the final microstructure is formed based on the quenching media. At high cooling rate, the whole  $\beta$  phase in the microstructure at solutionizing temperature converted to martensitic phase called  $\alpha'$  which is hard. During the cooling process at a slower cooling rate, for example, in the case of the samples cooled down in the air, some  $\beta$  phase converted to plate like  $\alpha$  phase and some grain boundary  $\beta$  phase. On the other hand, during rapid quenching of the samples solutionized under the  $\beta$  stability temperature, which two phases  $\alpha+\beta$  structure is formed, some primary  $\alpha$  phase is shown in the vicinity of  $\alpha'$ . The microstructure of the samples after the heat treatment cycles are shown in Fig. 1.

The microstructure of the as-received sample is presented in Fig. 1a, which contains primary  $\alpha$  phase in the vicinity of transformed  $\beta$  phase with fine  $\beta$  precipitates. As shown in Fig. 1b, for the

sample solutionized at 930°C and quenched in the air, primary  $\alpha$  is seen in the microstructure. Also, some  $\beta$  phase is converted to a mixture of  $\alpha+\beta$  called transformed  $\beta$ . This microstructure is similar to the as-received sample. For the sample solutionized at 930°C and quenched in the water, martensitic  $\alpha'$  phase appears near primary  $\alpha$  phase (Fig. 1c). In the case of samples solutionized at 1060°C, for the sample cooled down in the air, elongated  $\alpha$  phase and grain boundary  $\alpha+\beta$  mixed microstructure is seen in the microstructure (Fig. 1d). On the other hand, in the case of water quenched sample cooled down from 1060°C, fully martensitic microstructure is shown as previously mentioned (Fig. 1e). Fine  $\beta$  precipitates are seen in the aged samples as shown in Fig. 2. In fact, during the aging process the decomposition of  $\alpha'$  phase into  $\alpha$  and fine  $\beta$  precipitates occurs and this cause the precipitation hardening and so the hardness of the alloy increased after aging process.

As seen in Fig. 2, for the sample solutionized at 1060°C and air quenched, large grain boundary  $\beta$  phase in the form of laminated microstructure is formed in the microstructure.

Based on the results presented here, it seems that the holding time of 600 s was effective to achieve proper amount of partial or fully  $\beta$  phase in the solutionizing temperature. Also, the results of hardness after the aging process demonstrate that holding the samples for 360 s at the proper

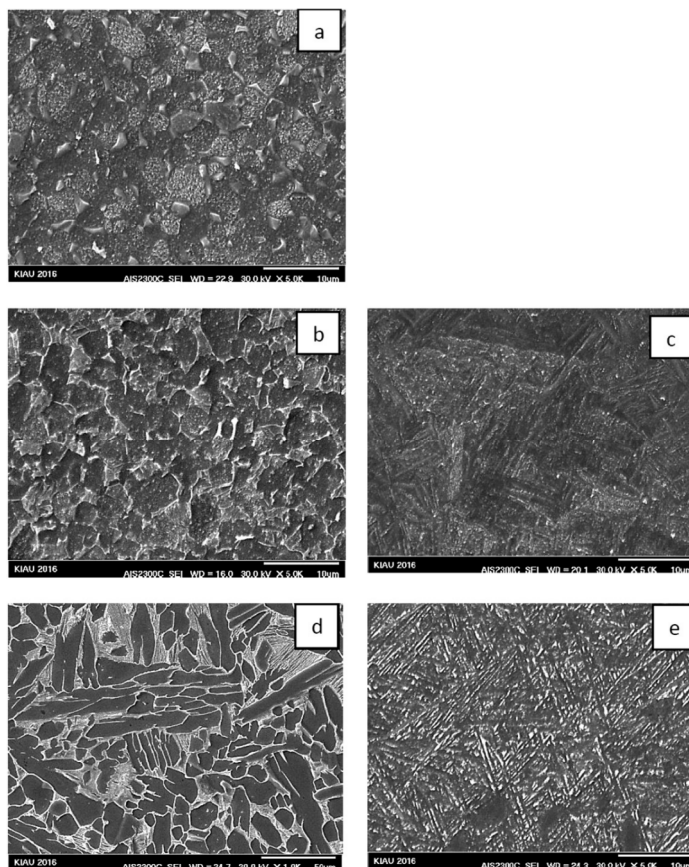


Fig. 1. The microstructure of the heat treated samples. a) As-received sample b) 930A550 c) 930W550 d) 1060A550 and e) 1060W550.

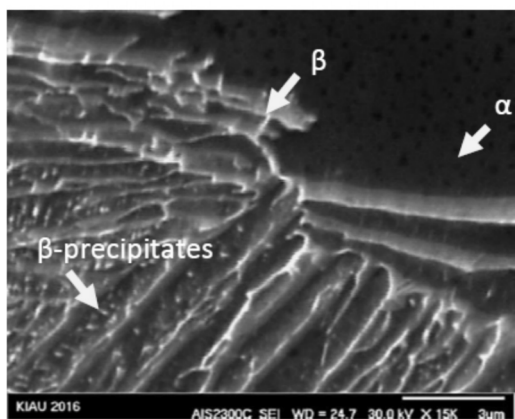


Fig. 2. Fine  $\beta$  precipitates formed during aging process at 550°C for 360 s.

aging temperature, was effective to increase the hardness of the material.

### 3. 2. Weight Loss and Wear Rate Results

Wear tests were applied on the samples with maximum hardness achieved in the aging process for each annealing temperature and quenching media. This situation occurs in the case of the samples aged at 550°C. The weight losses for the samples worn after 1000 m of sliding distance are depicted in Fig. 3. For all samples, increasing the applied load in wear test caused the weight loss to increase. Except for the sample air-cooled from 1060°C, there is a relation between the hardness and wear resistance of the sample. The best result for wear resistance is obtained in the case of the sample 1060W550. The micro mechanism of the

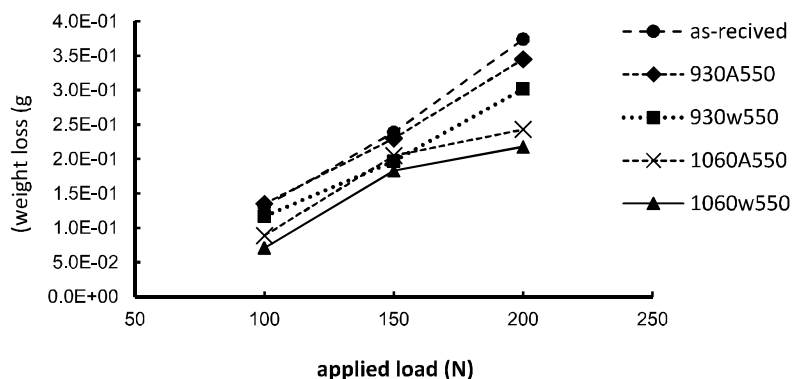


Fig. 3. The effect of applied load on weight loss of the samples after the wear test.

wear mechanism can be concluded using the evaluation of the worn surfaces of the pins and the debris formed during the wear test. Increasing the hardness value of the samples increases the resistance of surface deformation and so, the wear rate will be lessened. For the samples with low hardness value, the wear rate increases during the test as a result of low strength of the surface under the applied loads and contact between the pin samples and disc material.

The wear rates were calculated from the slope of the volume loss against sliding distance and plotted versus the applied normal load as illustrated in Fig. 4.

The specific wear rate,  $W_r$  ( $\text{mm}^3/\text{N m}$ ) was computed using Eq. (1) where,  $\Delta m$  is the weight

loss of the pin samples (g),  $\rho$  is the density of the test sample ( $\text{g}/\text{mm}^3$ ),  $t$  is the test duration (s),  $V_s$  is the sliding velocity (m/s),  $F_N$  is the average normal load (N).

$$W_r = \frac{\Delta m}{\rho t V_s F_N} \quad (1)$$

For all samples, the wear rate was increased gradually with the applied load. For the reference sample and for the samples solutionized at  $930^\circ\text{C}$  a transition was observed at the applied load of 150 N. In this case, there exists a transition from mild wear to severe wear at the loads higher than 150 N in this study. Same results have been

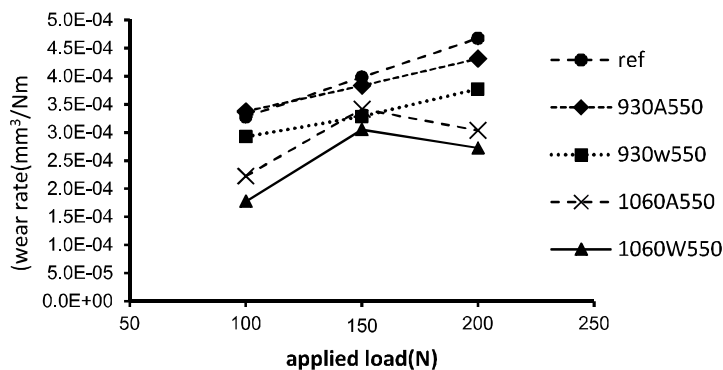


Fig. 4. The wear rate of the samples with different heat treatment applied on Ti-6Al-4V.

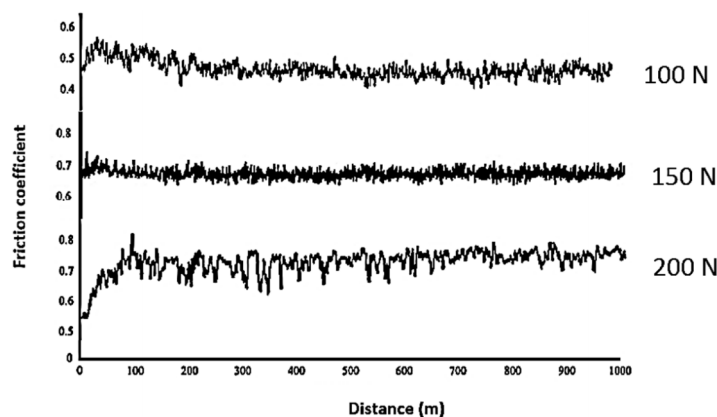


Fig. 5. Variation of friction coefficient with applied load.

reported by Ganesh et al [26]. For the samples annealed at 1060 °C the microstructure exhibited a lower weight loss. Despite the samples solutionized at 930 °C, there is a break down in the weight loss curve for the samples annealed at 1060°C. As shown in Fig. 4, for the samples solutionized at 930 °C the wear rate is increased with the applied load. But in the case of the samples solutionized at 1060 °C, the wear rate is decreased at the loads over 150 N.

Unexpectedly, for the sample cooled down from 1060°C in the air, the wear rate and the weight loss is less than the sample quenched from 930°C in the water which has higher hardness value. It may be related to the presence of coarse  $\beta$  phase in the microstructure (as indicated in Fig. 2), which caused the material to resist against wear. Further discussions about this unusual manner is kept out in the section 3.3 based on the worn surface examinations and microstructural investigations.

The average steady state coefficient of friction is plotted against the sliding distance for the samples in this study in Fig. 5. It was observed that the friction coefficient increased with applied load. In fact, by increasing the applied load, the adhesion of the contacting face is increased. So, the presence of adhesion between steel disc and titanium pin at high applied load is expected. Visual examination of the steel disc after the wear test in the case of the applied load higher than 150 N demonstrated the adhesion of pin material on the disc surface. For the as-received and the

samples solutionized at 930°C the adhesion sign on the disc material was noticeable in the case of applied load of 200N. It may be the main reason for the mild to severe wear transition for the as-received and the materials solutionized at 930°C which previously observed in Fig. 3 and 4.

### 3.3. Worn Surface Analysis

The results of microscopic examination of worn surfaces are shown in Fig. 6. The whole of the microstructures experienced considerable oxidation as demonstrated by the formation of material accumulation regions. The EDS elemental analysis revealed that the material accumulation regions were composed of Ti, O, V, Al, and Fe. The iron element entered from the disc material into the surface layers of the pin material. At the lowest applied load (100 N), SEM observations revealed that an oxidative wear mechanism is dominated for all the samples. Titanium and aluminum favored to form oxide compounds, specially at high temperatures. Friction induced heating at the surface of the pin caused the oxidation to increase. The oxide compounds are brittle and non-protective and so detached from the surface gradually and in this situation the rate of weight loss is low. For the samples with higher hardness, the oxidative wear mechanism is dominated at low applied loads. Even though the presence of abrasion grooves was evident on both worn surfaces, the samples quenched from 1060°C had smoother wear

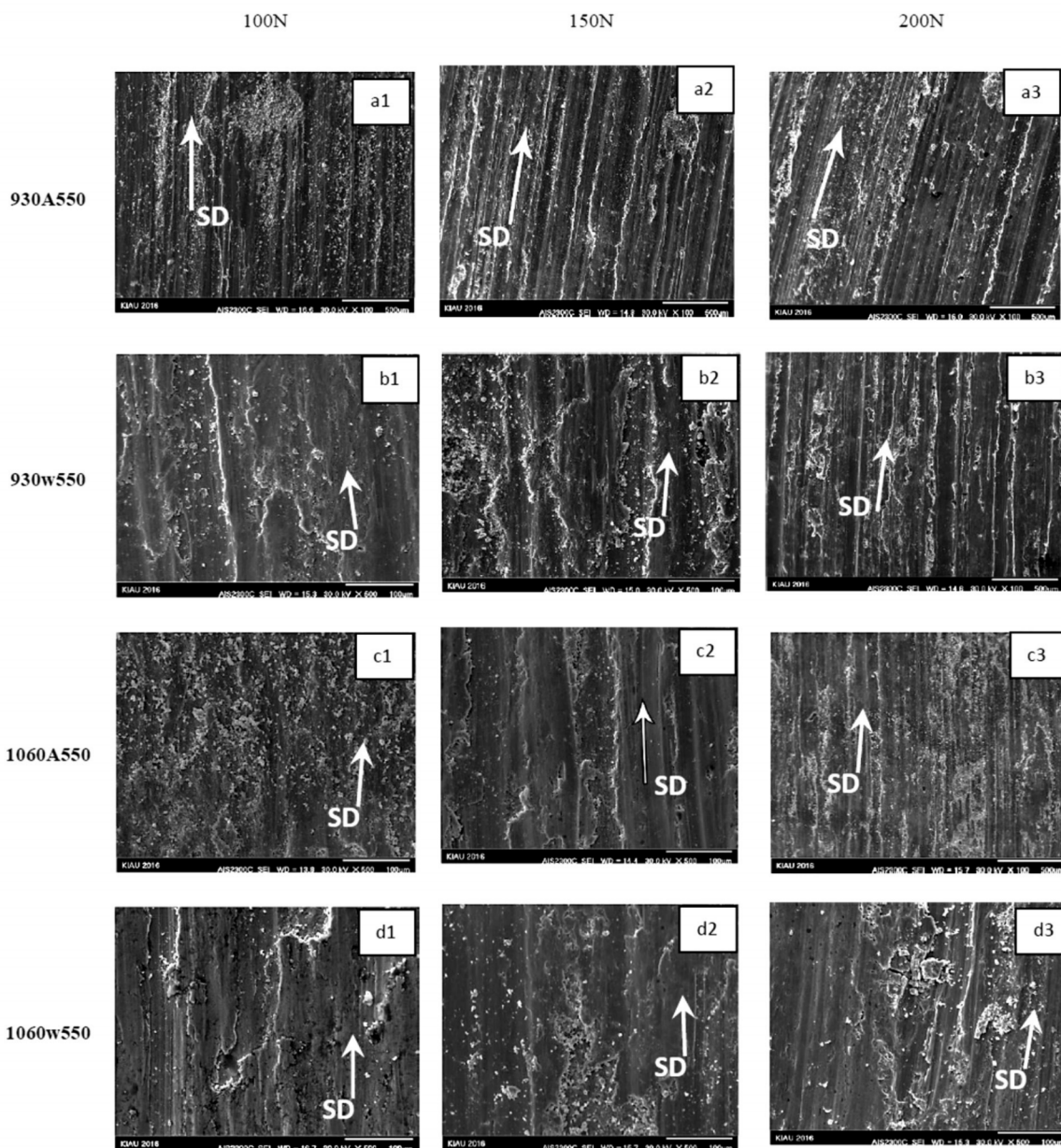


**Fig. 6.** SEM micrographs of worn surface of the samples in this study at different applied loads. a) 930A550 b) 930W550 c) 1060A550 and d) 1060W550. The indexes 1, 2 and 3 refer to applied load of 100, 150 and 200 N, respectively.

tracks.

Examination of the worn surface at higher magnifications revealed that there exist different wear micro mechanisms which contributed to the wear failure at different applied loads for the samples in this research. As shown in Fig. 7a, oxide particles are formed on the surface. As

mentioned previously, there is a great affinity for the titanium and aluminum element to oxidize during the wear of the Ti-6Al-4V alloy. So oxide particles will be formed on the wear tracks. Almost in all cases, fine oxide particles were seen on the surface of the worn samples. In the case of high applied load, oxide particles detached from

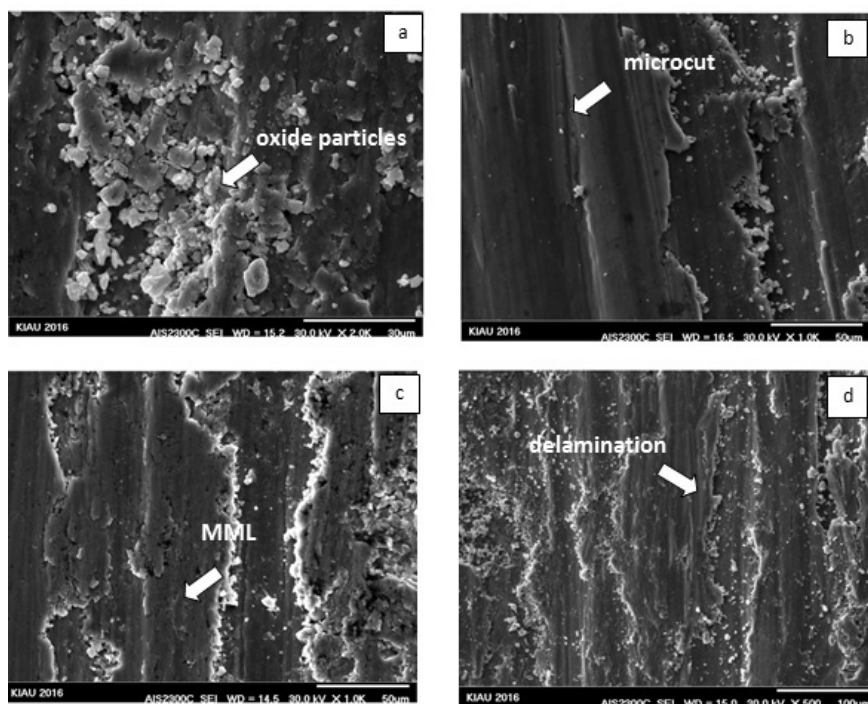


Fig. 7. SEM image of the worn surface shown wear micro mechanisms occurred for the samples in this research. a) Oxidation b) scratch and micro cutting c) MML formation d) delamination.

the surface and clean metallic surface can be seen on the pin.

Softer materials experienced severe signs of abrasion and cutting grooves at high applied load as shown in Fig. 7 b. In the case of high applied load of 200N, some mechanisms are active for all samples. At the contact point of the titanium pin and steel disc, a mechanically mixed layer (MML) will be formed. This layer is brittle in nature and so it may be detached from the surface. Also, the plastic deformation of the surface in the contact region will be occurred at high applied loads (200 N in this study) as it is shown in Fig. 7d. In this situation, delamination at the surface may be occurred. To examine the formation of MML and delamination on the surface of the pin material, SEM micrograph from the longitudinal cross section of the pin is shown in Fig. 8. As it is observed in Fig. 8a, deformation of the surface caused the sub-surface cracks and holes to form and grow up which elongated in the sliding direction. This discontinuity extended until a metal layer

detached from the surface and flake like debris of the substrate is formed. This is the delamination mechanism reported by Suh [17]. For the materials with higher hardness as well as higher strength, the occurrence of delamination mechanism is not dominated. So, the materials quenched in the water in this study, which have higher hardness value, are more wear resistant. As shown in Fig. 8 the flow pass of the material at the surface layer is presented by thin white arrows which represent the plastic deformation of the material in the sub-surface layers. Deformation of the surface resulted in the formation of sub-surface micro cracks and holes as mentioned previously and it is shown in Fig. 8a for the sample quenched from 930°C in the air. In comparison with the sample quenched in the air, the sample quenched in water has less plastic flow, which demonstrated that this material is more resistant to delamination.

On the other hand, the formation of mechanically mixed layer (MML) is seen on the surface of the material as shown in Fig. 8. EDS

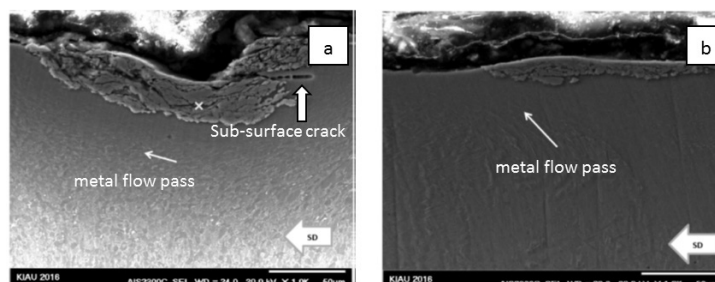


Fig. 8. SEM micrographs of under-worn surface of the samples in this study. a) 930°C air quenched and b) 930°C water quenched

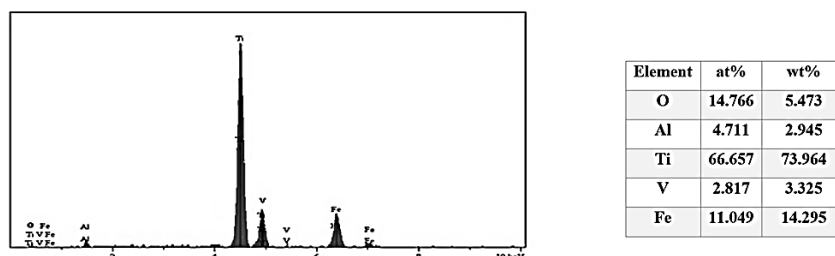


Fig. 9. EDS microanalysis results of MML layer formed on the worn surface.

microanalysis of the MML layer demonstrated the existence of iron in the chemical composition of this layer (Fig. 9).

As mentioned previously, for the sample cooled down from the 1060°C in the air, the alloy showed higher wear resistance even at high applied load in comparison with the sample water quenched from 930°C with higher hardness. For this sample, deformation at higher applied loads caused work hardening due to the presence of high volume fraction of  $\beta$  phase in the microstructure. So, the material will be more resistant to delamination in this situation.

When examined the debris under the SEM it was found that at different applied loads, there exist four types of morphologies. Wear debris may be consisted of loose, fine particles (Fig. 10a), micro cutting chips (Fig. 10b), metallic plate-like debris (Fig. 10c) and in the form of compacted particles (Fig. 10d). The EDS elemental analysis of the collected debris revealed the presence of Ti, O, V, Al, and Fe in

the compacted morphology debris which revealed that they may be composed of mechanically mixed compounds. However, the loose fine debris particles had higher oxygen content which means that they are composed of oxide particles.

After the introduction to the transition load in the samples with less hardness, shiny silver-colored appearance debris is observed in the visual inspections. The plate-like and micro-cutting chip debris were 300–600  $\mu\text{m}$  long and micro cracks were occasionally observed on their surfaces.

For softer materials, first signs of adhesion were observed at 150 N. By increasing the applied load, the ploughing and adhesion marks developed and expanded across the entire width of the wear track. Correspondingly, transferred material was detected on the steel disc. According to the elemental analysis the transferred material was composed of Ti, V, Al, and Fe. Subsequently, at higher loads adhesion

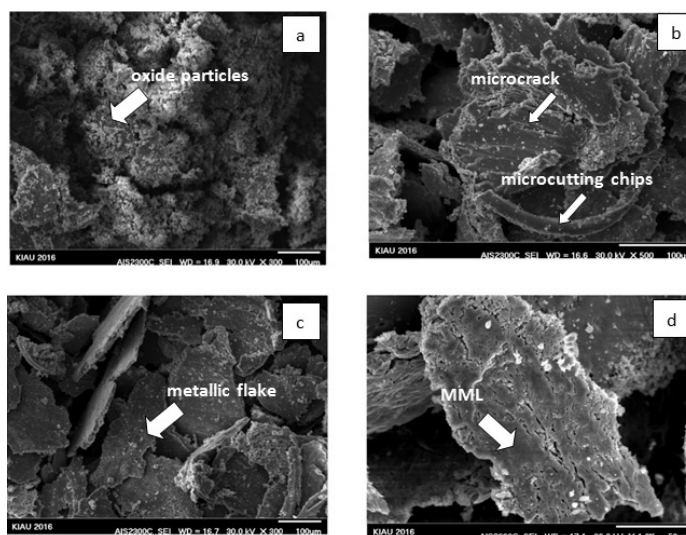


Fig. Types of debris created in the sliding wear of Ti-6Al-4V alloy.

was the main wear mechanism which caused mild to severe wear for the Ti-9Al-4V alloy solutionized at 930°C.

#### 4. CONCLUSIONS

The dry sliding wear behavior of Ti-6Al-4V alloy exposed to short holding time heat treatment at 930°C and 1060°C and tempering at 550°C against hardened 100Cr6 steel was studied and based on the results obtained in this study, the following conclusions can be stated:

1. Solutionizing Ti-6Al-4V at 930°C and 1060°C for short holding time of 600 s and aging them at 550°C for 360 s have great impact on the microstructure as well as the hardness of this alloy. When the samples are water quenched from the solutionizing temperature, the  $\beta$  phase, which formed due to the annealing in two phases ( $\alpha+\beta$ ) region at 930°C and in the fully  $\beta$  stabilized region at 1060°C transformed to  $\alpha'$  phase and so the hardness of the material would be increased. On the other hand, in the case of the samples cooled down in the air,  $\beta$  phase transformed to  $\alpha$  and some  $\beta$  precipitates which have lower hardness in comparison with the water quenched samples. Also, aging the samples caused some  $\alpha'$

converted to  $\alpha$  and  $\beta$  precipitates which additionally increases the hardness of the material.

2. At low applied load (100 N), SEM observations revealed that an oxidative wear mechanism is dominated for all the samples. Even though the presence of abrasion grooves was evident on both worn surfaces, the samples quenched from 1060°C had smoother wear tracks. Softer materials experienced severe signs of abrasion and cutting grooves at high applied load. A transition from mild to severe wear was observed for the samples solutionized at 930°C. Conversely, for the samples solutionized at 1060°C, the wear rate decreased with increasing the applied load. The samples cooled down from 1060°C revealed the maximum wear resistance, especially at high applied load. It may be contributing to the resistance to delamination wear mechanism which occurs in other samples at high applied loads.
3. There exist four types of debris observed with SEM examinations. They consist of fine oxides, cutting chips, metallic flakes produced via delamination and compacted mechanically mixed compounds. At the

contact point of the titanium pin and steel disc, a mechanically mixed layer (MML) will be formed at high applied load which contains high level of iron and oxygen. This layer is brittle and detached from the surface and produces compacted debris.

## REFERENCES

1. Chunxiang, C., BaoMin, H., Lichen, Z., Shuangjin, L., "Titanium alloy production technology, market prospects and industry development". *Mater. Design*, 2011, 32, 1684–91.
2. Budinski, K. G., "Tribological properties of titanium alloys", *Wear*, 1991, 151, 203–17.
3. Yerramareddy, S., Bahadur, S., "The effect of laser surface treatments on the tribological behavior of Ti–6Al–4V", *Wear*, 1992, 157, 245–62.
4. Morita, T., Asakura, K., Kagaya, C., "Effect of combination treatment on wear resistance and strength of Ti–6Al–4V alloy", *Mater. Sci. Eng. A*, 2014, 34, 438–446.
5. Grenier, M., Dubé, D., Adnot, A., Fiset, M., "Microstructure and wear resistance of CP titanium laser alloyed with a mixture of reactive gases", *Wear*, 1997, 210, 127–35.
6. Long, M., Rack, H., "Titanium alloys in total joint replacement", *materials science perspective. Biomaterials* 1998, 19, 1621–39.
7. Agins, H. J., Alcock, N. W., Bansal, M., Salvati, E., Wilson, P. O., Pellicci, P., "Metallic wear in failed titanium-alloy hip replacements", *J. Bone Joint Surg.*, 1988, 170A(3), 347–56
8. Yang, H., Gao, P. F., Fan, X. G., Li, H. W., Sun, Z. C., Li, H., Guo, L. G., Zhan, M., Liu, Y. L., "Some advances in plastic forming technologies of titanium alloys", *Procedia Engineering*, 2014, 81, 44 – 53.
9. Molinari, A., Straffelini, G., Tesi, B., Baccari, T., "Dry sliding wear mechanism of the Ti6Al4V alloy", *Wear* 1997, 208, 105–12.
10. Straffelini, G., Molinari, A., "Dry sliding wear of Ti–6Al–4V alloys influenced by the counter face and sliding conditions", *Wear*, 1999, 236, 328–38.
11. Alam Ohidul, M., Haseeb, A., "Response of Ti–6Al–4V and Ti–24Al–11Nb alloys to dry sliding wear against hardened steel", *Tribol. Int.*, 2002, 35, 357–62.
12. Dong, H., Bell, T., "Tribological behavior of aluminum sliding against Ti6Al4V in unlubricated contact", *Wear*, 1999, 225, 874–84.
13. Qiu, M., Zhang, Y. Z., Zhang, J. H., Zhu, J., "Microstructure and tribological characteristics of Ti–6Al–4V alloy against GCr15 under high speed and dry sliding", *Mater. Sci. Eng.*, 2006, 43A, 71–5.
14. Magaziner, R. S., Jain, V., Mal, S., "Investigation into wear of Ti–6Al–4V under reciprocating sliding condition", *Wear*, 2009, 267, 368–73.
15. Manisavagam, G., Amritpreet, K. S., Rajamanickam, A., Ashok, K. G., "Ti based biomaterials: the ultimate choice for orthopaedic implants – a review", *Progress in Mater. Sci.*, 2009, 54, 397–425.
16. Pinke, P., Reger, M., "Heat Treatment of the cast Ti–6Al–4V Titanium Alloy", *Proceedings of 12th International Scientific Conference COMAT-TECH*, 2004, 1042–1046.
17. Morita, T., Hatsuoka, K., "Strengthening of Ti–6Al–4V Alloy by Short time Duplex Heat Treatment", *Materials Transactions*, 2005, 46, 1681–1686.
18. Carreon, H., Ruiz, A., Santovena, B., "Study of Aging Effects in a Ti–6Al–4V Alloy with Widmanstätten and Equiaxed Microstructures by Non-Destructive Means", *AIP Conference*, 2014.
19. John, J., Nagarajan, N. M., "Age hardening Treatment of Ti–6Al–4V alloy dome for Aerospace Application", *Int. J. Innovative Sci. Eng. Technol.*, 2015, 2, 45–52.
20. Khanna, N., Garay, A., "Effect of Heat Treatment Conditions on Machinability of Ti–6Al–4 and Ti–5Al–2.5Sn alloys", *Fifth CIRP Conference on High Performance Cutting*, 2012, 255–260.
21. Chandler, H., "Heat treatment's guide—Practices and Procedures for Nonferrous Alloys", *ASM International*, 2006, 522–536.
22. ASTM F 136, "Standard Specification for Wrought Titanium–6Aluminum–4Vanadium ELI (Extra Low Interstitial) Alloy for Surgical Implant Applications (UNS R56401)"
23. Devaraya, G., Shetty, R., Rao, Sh., Gaitonde, V.,

- “Wear resistance enhancement of titanium alloy(Ti-6Al-4V) by ball burnishing process”, *J. Mater. Proces. Technol.*, 2016, Article in press.
24. Suh, N., “The delamination theory of wear”, *Wear*, 1973, 25, 111-24.
  25. Ganesh, B., Ramaniah, N., Chandrasekhar Rao, P., “Dry Sliding Wear Behavior of Ti-6Al-4V Implant Alloy Subjected to Various Surface Treatments”, *Transactions of the Indian Institute of Metals*, 2012, 65, 425-434.
  26. Ganesh, B., Ramaniah, N., Chandrasekhar Rao, P., “Effect of heat treatment on dry sliding wear of titanium-aluminum-vanadium (Ti-6Al-4V) implant alloy”, *J. Mech. Eng. Research*, 2012, 4, 67-74.